**ISSN: 2582-8118** ***Volume 1, Issue 4; July 2021***

INTERNATIONAL JOURNAL OF RESEARCH AND ANALYSIS IN SCIENCE AND ENGINEERING

Web: https://www.iarj.in/index.php/ijrase/index

# 6. A Study on Modulation Method with Reference to Optical Fiber

**Dr. P. K. Jha**
*Associate Professor,*
*Dept. of Physics, M. L. S. M. College, Darbhanga, Bihar.*

**Prof. Madan Kumar Mahto**
*Dept. of Physics, K. S. R. College, Sarairanjan, Samastipur.*

***ABSTRACT***

*For the transfer of the binary waveform, Modulation of amplitude (AM), modulation phase (MP) or modulation of frequencies (FM) can be utilized when it is necessary for a carrier to superimpose. Also often used are combination systems like AM-PM modulation of amplitude (MA).*

***KEYWORDS***

*Optical Fiber, Binary Phase, Shift Keying, BPSK, BPSK Signals.*

## Introduction:

A declining channel in which the received signal amplitude differs over time due to transmission medium variabilities. FM is useful when contending with such channels and is relatively unreliable to amplitude fluctuations. In each case, we must have a transmitter modulator and a demodulator at the receiver to retrieve the signal of the baseband. This combination of modulator and demodulator is known as a MODEM. This chapter describes and compares many of the available modulation / demodulation techniques based on their spectrum occupancy.

## Review of Literatures:

Many Current 40 gbit s was concentrated in research and development –When external laser modulation is necessary for transmission, as an instance, an electro absorption modulator or a Mach–Zehnder [1-14, 15]. This factor additionally especially for single-mode fibres, it is helpful in the first longer wavelength window region at 1.3 gm, when fibre intramodal dispersion is lowest and transmission bandwidth is maximized.

It's also worth noting that, following a preliminary area trial demonstration in 1982 [16], this fibre type quickly started to dominate system packages inside tele-communications. Furthermore, the lowest silica glass fiber losses thus far of zero.1484 db km-1 were stated in 2002 for the opposite greater wavelength window at 1.57 gm [17] however, alas, chromatic dispersion is greater at this wavelength, for this reason restricting the maximum bandwidth conceivable with traditional unmarried-mode fiber. To gain low loss over the complete longer wavelength fibre transmission region from 1.3 to at least one.6 gm, or as an alternative, very low loss and occasional dispersion on the equal operating wavelength of normally 1.Fifty-five gm of superior unmarried systems of fibre, namely low water top and non-zero dispersion shifted fibre, had been commercially realized. Although features in the fibre era continued quickly in the past years, some previously preferred hobby regions include the fluoride fibre software to operate in the centre of infrarot even longer (2 to 5 pm) Far-infrared areas (8 to 12 pm) have decreased due to failure to show the theoretically predicted extremely low losses in fibre, combined with the development of the optical amps for use with fibres mainly based on silica. [11-17]

## Binary Phase-Shift Keying:

The data is in a single phase and the phase is 180° when the data is in a different level. The sinusoid has an amplitude capacity The Faithful

$= \frac{1}{2}A^2$ so that $A = \sqrt{2P_s}$ . So the signal is transmitted

$$\upsilon_{BPSK}(t) = \sqrt{2P_s}\cos(\omega_0 t) \quad (1.1)$$

or $$\upsilon_{BPSK}(t) = \sqrt{2P_s}\cos(\omega_0 t + \pi) \quad (1.2)$$

$$= \sqrt{2P_s}\cos(\omega_0 t) \quad (1.3)$$

A binary digit strip with voltage is included in BPSK data b (t), it's logical level 1, And 0 when b (t) = 1V is the logical level. We say its logical level. Therefore, as no loss of generality, the word BPSK (t) can be written

$$\upsilon_{BPSK}(t) = b(t)\sqrt{2P_s}\cos(\omega_0 t) \quad (1.4)$$

In practice, the waveform cos 0t as a carrier is generated to the equilibrated modulator and the Baseband signal b (t) is applied as the modulating waveform. A BPSK signal is produced as a practical BPSK by the waveform cos 0t for the balanced modulator, and the baseband signal b (t) as modulatory waveform.

## Reception of BPSK:

The signal received has the shape,

$$\upsilon_{BPSK}(t)=b(t)\sqrt{2P_s}\cos(\omega_0 t+\theta)=b(t)\sqrt{2P_s}\cos\omega_0(t+\theta/\omega_0) \quad (1.5)$$

Here θ is a nominally fixed Shift in phase that matches the downtime$\theta/\omega_0$It depends on the transmitter path length to the recipient and the shift in phase of the amplifiers at the front end of the pre-demodulator recipient. [18, 19-23]

In the demodulator the original b (t) data is retrieved. The demodulation usually used approach is called synchronous demodulation and requires the availability at demodulator the waveform cos ($\omega_0$t+θ). In Figure 1.1 there is a system to generate the carriers on the demodulator and to recover the signal of the baseband.

To generate the signal the incoming signal is squared

$$\cos^2(\omega_0 t+\theta)=\frac{1}{2}+\frac{1}{2}\cos 2(\omega_0 t+\theta) \quad (1.6)$$

The dc components are removed from the band-pass filter with a centred band about 2f0 and a signal with a waveform of cos 2 2($\omega_0$t + θ) is sent to us. The wavelength cos ($\omega_0$t + θ) is regenerated by a frequency divider (consisting of a filter flip-flop and a narrow-band filter f0). Accordingly in Figure 1.1 All amplitudes we took to be unity arbitrarily. The amplitudes of this equipment are defined in practice by characteristics that are not presently relevant.

When the carrier has been recovered, the received signal is amplified in any case.

$$b(t)\sqrt{2P_s}\cos^2(\omega_0 t+\theta)=b(t)\sqrt{2P_s}\left[\frac{1}{2}+\frac{1}{2}\cos 2(\omega_0 t+\theta)\right] \quad (1.7)$$

This is subsequently applied as indicated in Figure 1.1 to the integrater.

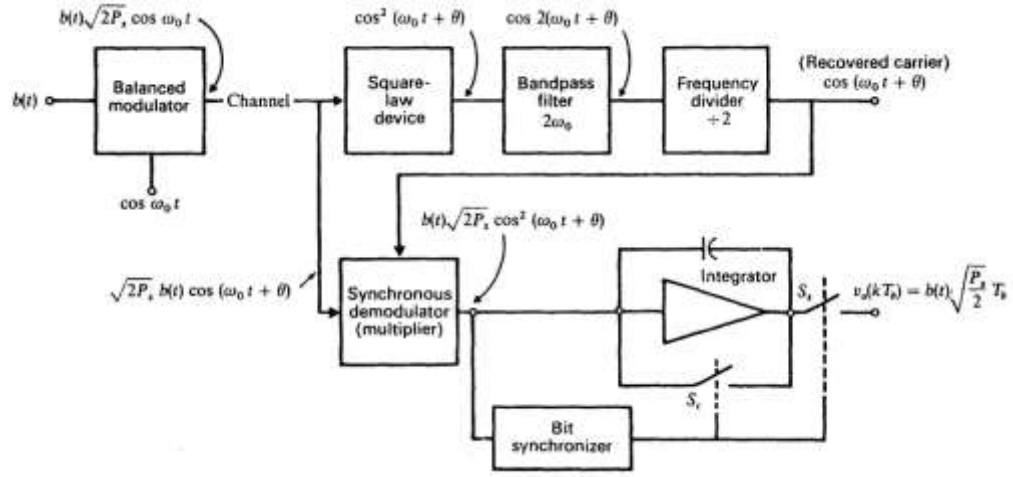


**Figure 1.1: Scheme to recover the baseband signal in BPSK**

In this scenario, the output voltage $\upsilon_{\upsilon}$,($kT_b$) extends from time (k-1) $T_b$, to $kT_b$, employing Eq. 1.7 at the end of a bit interval

$$\upsilon_{\upsilon}(kT_b) = b(kT_b)\sqrt{2P_s}\int_{(k-1)T_b}^{kT_b}\frac{1}{2}dt + b(kT_b)\sqrt{2P_s}\int_{(k-1)T_b}^{kT_b}\frac{1}{2}\cos 2(\omega_0 t+\theta)dt \qquad (1.7)$$

$$= b(kT_b)\sqrt{\frac{P_s}{2}}T_b \qquad (1.8)$$

Because a sinusoid integral has a zero value for an entire number of cycles. So our system reproduces the transmitted bit stream b (t) at the demodulator output.

**BPSK Spectrum:**

The b (t) shape is a binary NRZ shape (non-return-to-zeto) with a power spectral density of + $\sqrt{P_s}$ to– $\sqrt{P_s}$ for a wave shape. We've got

$$G_b(f) = P_s T_b\left(\frac{\sin\pi f Tb}{\pi f Tb}\right)^2 \qquad (1.9)$$

The NRZ waveform, multiplied by $\sqrt{2}$ cos $\omega_0$ t, is the BPSK waveform. Thus, after examination of Sec. 3.2, we observe that the BPSK signal is of Spectral power density.

$$G_{BPSK}(F) = \frac{P_s T_b}{2}\left\{\left[\frac{\sin\pi(f-f_0)T_b}{\pi(f-f_0)T_b}\right]^2 + \left[\frac{\sin\pi(f-f_0)T_b}{\pi(f-f_0)T_b}\right]^2\right\} \qquad (1.10)$$

Equations (1.9) and (1.10) are plotted in Figure 1.2.

**Geometrical Representation of BPSK Signals:**

In terms of orthonormal signal, we note that there can be a BPSK signal described $u_l$ (t) = $\sqrt{(2/T_b)}$ cos $\omega_0$t as ---------- (2.1)

$$\upsilon_{BPSK}(t) = \left[\sqrt{P_s T_b}b(t)\right]\sqrt{\frac{2}{T_b}}\cos\omega_0 t = \left[\sqrt{P_s T_b}b(t)\right]u_0(t) \qquad (1.11)$$

The PSK binary signal can be drawn as illustrated in figure 1.3. The gap between the pulses is noteworthy

$$d = 2\sqrt{P_s T_b} = 2\sqrt{E_b} \tag{1.12}$$

Where $E_b = P_s T_b$ is a bit-duration energy. In Sec. 11.13 we showed,

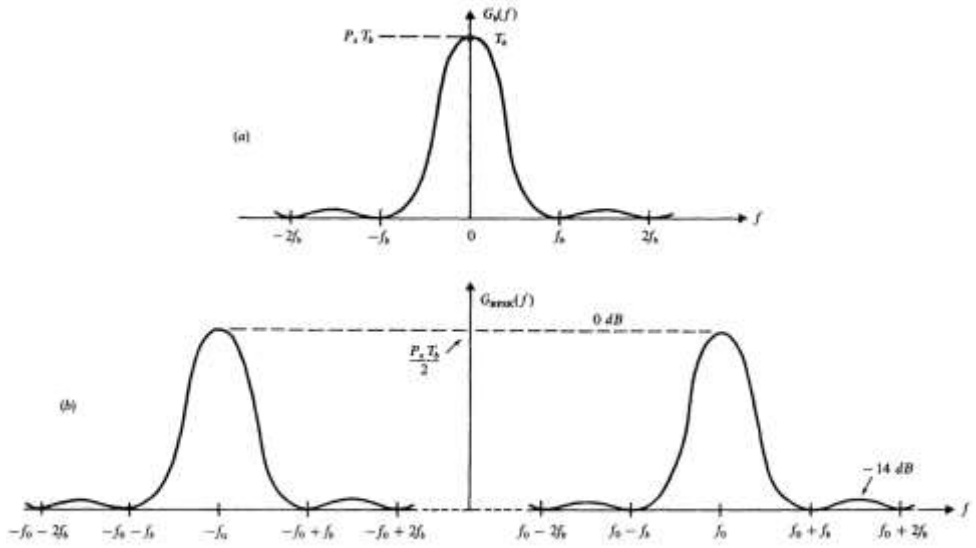

**Figure 1.2 (a) NRZ data spectral power density b (t). (b) Power spectral density of binary PSK**

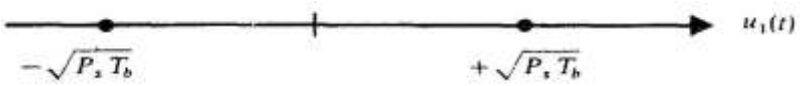

**Figure 1.3: Geometrical representation of BPSK signals**

When trying to determine which level of b (t) is received in case of noise, distance d is inversely linked to the risk of making a mistake.

**2.3 Differential Phase-Shift Keying:**

In Figure 6.1, we noted that we are starting in squaring b (t) $\sqrt{2P_s}$ cos $\omega_0 t$ to regenerate the transport in BPSK. Consequently, the requested carrier would remain the same if it were instead a signal –b (t) $\sqrt{2P_s}$ cos $\omega_0 t$.

Therefore we cannot identify if the broadcast signal b (t) or its negative –b (t) is the received baseband signal.

A mechanism is shown in Figure 1.4 to generate a DPSK signal. D (t) is used to provide an exclusive OR logic gate entry to the transmitted data stream.

Once the Tb is allocated for one bit, b (t) is delayed with the exclusive output or gate.

The top level of the shape of the wave is Logic 1 and the bottom is Logic 0. Figures 1.4 shows the table of truth for the exclusive OR gate

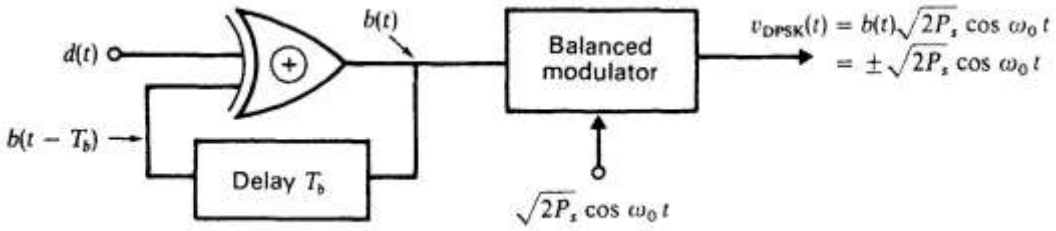


| d(t) | | b(t − $T_b$) | | b(t) | |
|---|---|---|---|---|---|
| logic level | voltage | logic level | voltage | logic level | voltage |
| 0 | −1 | 0 | −1 | 0 | −1 |
| 0 | −1 | 1 | 1 | 1 | 1 |
| 1 | 1 | 0 | −1 | 1 | 1 |
| 1 | 1 | 1 | 1 | 0 | −1 |

**Figure 1.4: Means of DPSK signal generation**

No. of Interval

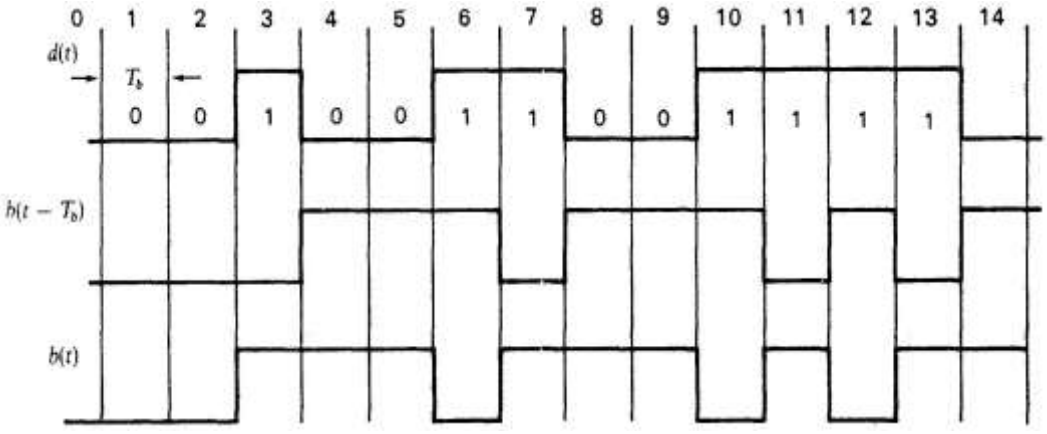


**Figure 1.5: Logical waves to show the answer b (t) to the input d (t)**

And We Can Simply Confirm From This Table That Each Waveform Is Consistent With B (T–Tb), D (T) And B For Each Other (T). In Fact, B (T–Tb) Is Delayed For One Bit, And B(T) Is Delayed For Each Bit Interval, And B(T) = D [T] = B(T–Tb).The Symbolism D(K) B(K) And D(T) Are Used During The Kth Period In The Following Discussion To Represent The Logic Levels Of D(T) And B(T).

Due To The Feedback In The System Logical Levels Of Our Interval In The Drawing Of The Wave Forms Are Somewhat Difficult To Identify (Interval 1 In Figure 1.5).

Now We Observe That At The Beginning Of Each Interval, The B (T) Reaction To D (T), B (T) Changes Level, Where D (T) = 1 And B (T), When D (T) = 0, Don't Change Levels. Thus D (3) = 1 Changes At the Beginning of Period 3, and At That Interval, B (3) Changes. At Intervals 6 And 7, Change D (6) = D (7) = 1 and Change B (T) At the Beginning of the Two. At The Beginning of Each Intervals There Are B (T) Modifications in B (10, 11, 12 And 13 D (T) = 1. This Conduct Is Expected From An Exclusive OR Gate's Truth Table. It Should Be Pointed Out That, If D (T) = 0, B (T) = B (T – $T_b$) It Will Duplicate Itself Irrespective Of The Original Value Of B (T – $T_b$). In D (T) = 1 on the Other Hand, B (T) = $b(t-T_b)$ Changes Its Preceding Interval Valueat Each Consecutive Bit Interval. Note: We Have B(T) = 0 At Interval D(T) = 0 In Interval D(T), And B(T) = 1, At Other Interval D(T) = 0. Likewise, If D (T) = 1 B (T) = 1 At Times, And B (T) = 0 at Times. So, No Relationship Between The D(T) And B(T) Levels, And The System's Only Invariant Function Is That Changes In B(T) Occur When D(T)=1, Sometimes Up And Down, And No Change In B(T) Occurs Whenever D(T) = 0.

In Addition, In Interval 1, B (0) = 0, The Shapes Of Figure 1.2 Are Assumed. If We Assume B (0) =1, We Shall Continue To Apply The Invariant Feature By Which The System Is Characterized, If Not Immediately Obvious, As Is Easily Confirmed. Since Either B (0) = 0 Or B (0) = 1 Has To Be Either B (0), There Are No Further Options, Our Solution Is Generally Valid. However, If We Had Begun B (0) = 1, We Would Have Reversed Levels B (1) And B (0). As Can Be Observed From Figure 1.1 B (T) Shall Be Used For A Balanced Module For The Carrier $\sqrt{2P_s}\cos\omega_0 t$ Is Also Applied. The Output of the Modulator, the Signal Is Sent

$$\begin{aligned} \upsilon_{DPSK}(t) &= b(t)\sqrt{2P_s}\cos\omega_0 t \\ &= \pm\sqrt{2P_s}\cos\omega_0 t \end{aligned} \tag{1.13}$$

So If D (T) = 0, At the Beginning of the Bit Interval, the Carrier's Phase Does Not Change, But D (T) = 1 Changes Magnitude = M.

Here, The Signal Received Is Put To A Multiplier And The Signal Received Is Delayed By The Bit Time Tb. The Output Is Multiplier

$$\begin{aligned} & b(t)b(t-T_b)(2P_s)\cos(\omega_0 t+\theta)\cos[\omega_0(t-T_b)+\theta] \\ &= b(t)b(t-T_b)P_s\left\{\cos\omega_0 T_b+\cos\left[2\omega_0\left(t-\frac{T_b}{2}\right)+2\theta\right]\right\} \end{aligned} \tag{1.14}$$

And Applied In Figure 1.1 Demodulator For Bpskto The Bit Synchronizer And Integrator. We Should Select $\omega_0$ $T_b$ So That $\omega_0$ $T_b$ = 2nπ with N an Integer. For In This Scenario, the Signal Output Will Be As Large As Feasible With Cos $\omega_0$ $T_b$ = + 1

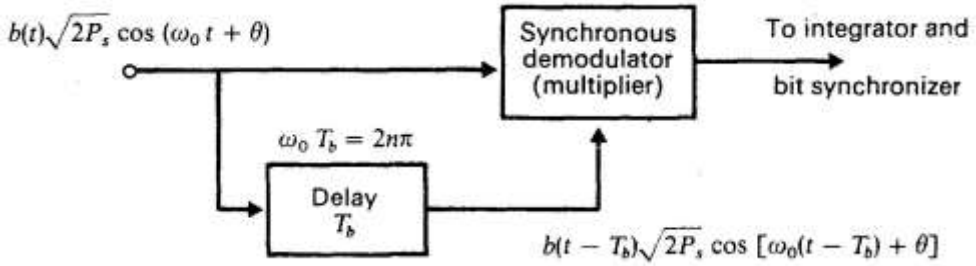


**Figure 1.6: Data recovery method of DPSK signal. Data recovery method**

Furthermore, the duration of the bit consists of an integrated number of clock cycles, and the integrated term is zero exactly. [19-27] the data bit d (t) transferred B (t) b (t –Tb) of the product can be readily computed.

## Differentially-Encoded PSK (DEPSK):

Synchro demodulation recovers the signal b (t) in this system and b (t) decoding is performed on the baseband to obtain d (t).

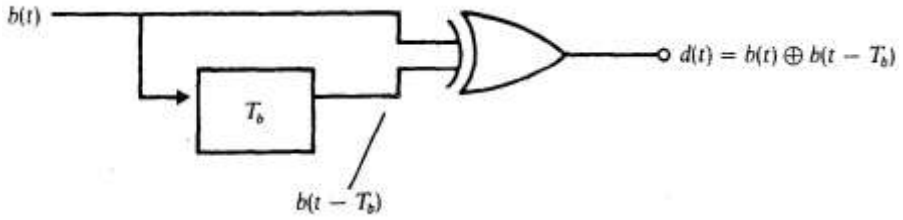


**Figure 1.7: Decoder for the baseband to get d (t) from b (t).**

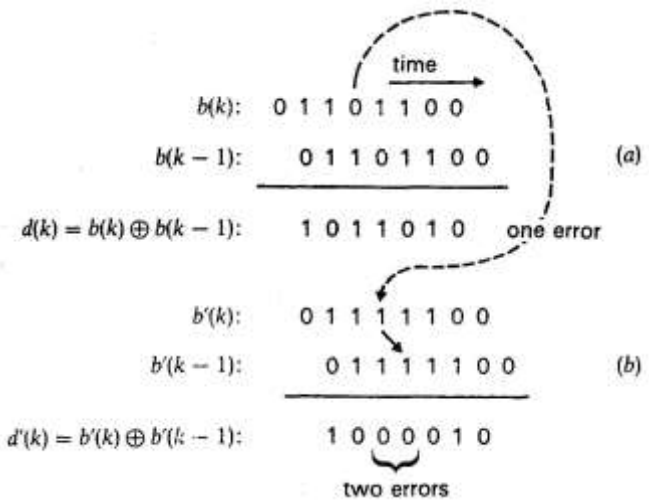


**Figure 1.8: Errors occur in couples with variably encoded PSK**

In Figure 1.1, the DEPSK transmitter is identical to the DPSK System transmission. The signal b (t) for a BPSK system is retrieved in the same manner as described in Figure 1.1.

This message is then transmitted directly into an OR logical gate input and the second is applied with b (t - Tb) (see Figure 1.7). Gate output is at the same level whether b (t) = b (t – $T_b$) or b (t) = $\overline{b(t-T_b)}$. The first time is b (t) and the delivered bit is therefore d (t) = 0. In the 2 situation d (t) = 1.

## Discussion:

If we make a mistake in this chapter, then mistakes must emerge from a comparison with the previous and successful part. Figure 1.8 shows this outcome.

We suppose in Figure 1.8b that b'(k) has one single mistake. There is then a single mistake for b'(k – 1).

## References:


1. F. P. Kapron et al., 'Radiation losses in glass optical waveguides', *Appl. Phys. Lett.*, vol. 17, no. 10, pp. 423-425, 1970.
2. IEEE 802.3-2002, 'Information Technology- Telecommunication & Information Exchange between Systems - Local and Metropolitan Area Networks – Specific Requirements, Part 3: Carrier Sense Multiple Access with Collision Detection (CSMA/CD) Access Method and Physical Layer Specifications 2002'.
3. TIA/EIA-455-203 (2001), FOTP-203 - Launched Power Distribution Measurement Procedure for Graded-Index Multimode Fibre Transmitters
4. TIA/EIA-455-54-B (2001), 'FOTP-54 - Mode Scrambler Requirements for Overfilled Launching Conditions to Multimode Fibers'
5. TIA/EIA-455-204 (2000), 'FOTP-204 - Measurement of Bandwidth on Multimode Fibre.
6. J. B. Schlager et al., 'Measurements for Enhanced Bandwidth Performance Over 62.5 um Multimode Fibre in Short-Wavelength Local Area Networks', *IEEE J. Lightwave Technol.*, vol. 21, no. 5, pp. 1276-1285, 2003.
7. TIA-455-220-A (2003), 'FOTP-220 - Differential Mode Delay Measurement of Multimode Fibre in the Time Domain'
8. TIA-492AAAC-A (2003), 'Detail Specification for 850-nm Laser-Optimized, 50- um Core Diameter/125-um Cladding Diameter Class Ia Graded-Index Multimode Optical Fibres'
9. P. Pepeljugoski et al., 'Development of System Specification for Laser-Optimized 50 um Multimode Fibre for Multigigabit Short-Wavelength LANs', *IEEE J. Lightwave Technol.*, vol. 21, no. 5, pp. 1256-1275, 2003.
10. L. Raddatz et al., 'Influence of restricted mode excitation on bandwidth of multimode fibre links', *IEEE J. Photon. Technol. Lett.*, vol. 10, no. 4, pp. 534- 536, 1998.
11. L. Raddatz et al., 'An experimental and theoretical study of the offset launch technique for the enhancement of the bandwidth of multimode fibre links', *IEEE J. Lightwave Technol.*, vol. 16, no. 3, pp. 324-331, 1998.

12. ISO/IEC14763-3 (2006), 'Information technology — Implementation and operation of customer premises cabling — Part 3: Testing of optical fibre cabling'.
13. R. Olshansky and D. A. Nolan, 'Mode-dependent attenuation of optical fibres: excess loss', *Appl. Opt.,* vol. 15, no. 4, pp. 1045-1047, 1976.
14. M. Y. Loke and J. N McMullin, 'Simulation and measurement of radiation loss at multimode fibre macrobends', *IEEE J. Lightwave Technol.,* vol. 8, no. 8, pp. 1250-1256, 1990.
15. D. Gloge, 'Bending Loss in Multimode Fibres with Graded and Ungraded Core Index', *Appl. Opt.,* vol. 11, no. 11, pp. 2506-2513, 1979.
16. K. Kitayama et al., 'Impulse Response Prediction Based on Experimental Mode Coupling Coefficient in a 10-km Long Graded-Index Fibre', *IEEE J. Quantum Electron,* vol. 16, no. 3, pp. 356-362, 1980.
17. J. M. Senior, "*Optical Fibre Communications*", section 2.3, Prentice Hall, second edition, 1992.
18. D. Gloge, 'Weakly Guiding Fibres', Appl. Opt., vol. 10, no. 10, pp. 2252-2258, 1971.
19. 24. M. J. Adams et al., 'Leaky rays on optical fibres of arbitrary (circularly symmetric) index profiles', Electron. Lett., vol. 11, no. 11, pp. 238-240, 1975.\
20. R. Olshansky, 'Leaky modes in graded index optical fibres', Appl. Opt., vol. 15, no. 11, pp. 2773-2777, 1976.
21. F. Sladen et al., 'Determination of optical fibre refractive index profiles by a near-field scanning technique', Appl. Phys. Lett., vol. 28, no. 8, pp. 225-258, 1976.
22. Y. Daido et al., 'Determination of modal power distribution in graded-index optical waveguides from near-field patterns and its application to differential mode attenuation', Appl. Opt., vol. 18, no. 13, pp. 2207-2213, 1979.
23. O. G. Leminger and G. K. Grau, 'Near-field intensity and modal power distribution in multimode graded-index fibres', Electron. Lett., vol. 16, no. 17, pp. 678-679, 1980.